

Implementation of Soil Lateral Pressure Measurement due to Vehicle Under Constant Speed Based on LabVIEW Software

Iman Handiman
Department of Civil Engineering
Faculty of Engineering,
Siliwangi University
Tasikmalaya, Indonesia
imanhandiman@unsil.ac.id

I Wayan Redana
Department of Civil Engineering
Faculty of Engineering,
Udayana University
Denpasar, Indonesia
iwayanredana@yahoo.com

Anissa Maria Hidayati
Department of Civil Engineering
Faculty of Engineering,
Udayana University
Denpasar, Indonesia
anissamh@unud.ac.id

I Ketut Sudarsana
Department of Civil Engineering
Faculty of Engineering,
Udayana University
Denpasar, Indonesia
ksudarsana@unud.ac.id

Abstract— The weight of the vehicle should be able to reflect the magnitude of the horizontal pressure that occurs on the ground being passed. However, until now practically the calculation of lateral earth pressure on the roadside is still calculated from the static load which is considered equivalent. Therefore, this study aims to provide a simple formula for calculating lateral stresses caused by vehicles at constant speed. Measurements were made by recording the lateral pressure in real time using the load cell sensor system and the LabVIEW NI (National Instrument) processing unit, with a reading of $\pm 0.02\%$. Data collection was carried out through observation and the results showed that the greatest effect occurred when the load position was at the closest distance to the monitoring device. The monitored stress distribution is quite in line with the Boussinesq approach to static loads. The lateral stresses that occur are compared with the results of the Boussinesq formula for a constant load is about 0.003 times. However, further research still needs to be done to obtain the exact relationship formula between vehicle weight and the amount of pressure when running at a constant speed.

Keywords— *boussinesq, dynamic load, Labview, lateral pressure, load cell*

I. INTRODUCTION

The process of determining the response rate of the soil medium in moving vehicles has received considerable attention in the past. The finished retaining wall along road side will be loaded by heavy traffic on a roadway situated just behind the crest [1]. The observed movement can be interpolated between the values for K_a and K_o to estimate the actual pressure being applied to the retaining wall [2][3]. In the modeling analysis, the traffic load can be modeled using the wheel contact area which represents the axle load [4]. However, lateral overload is not only caused by traffic but also by the weight of saturated soil [5]. Retaining walls generally rarely have problems that are directly related to the bearing capacity of the soil but are more critical of horizontal or lateral pressure so that in this study the magnitude of the bearing capacity of the soil will not be discussed. Therefore, this research was motivated by the need to determine the vibrational motion of moving vehicles at the soil level and the associated depth due to pressure exerted on the road [6]. Dynamic loads on soil come from earthquakes, bomb

explosions, machine and construction operations, mining, traffic, wind, and wave action [7]. The part of the road that stretches through the slope or close to vertical is supported by soil retaining walls, cantilever pile walls, bulkheads, and braced pieces. Therefore, the soil lateral pressure needs to be properly calculated to obtain the right structure for the design [8]. Furthermore, the edge of the foundation is likely to experience a greater settlement than the center. This process occurs because the soil located at the foundation's edge does not have lateral confining pressure and therefore has a lower strength [9].

Determination of soil stress caused by machine traffic requires the use of properly installed tension transducers at different depths and distances from the wheel centerline [5]. This is because the soil generally consists of several layers with varying properties [10]. However, not all layers consist of ideal elastic materials therefore, within certain limits, they are still considered elastic media [11]. Comparison between viscoelastic and poroviscoelastic models shows that they both have similar displacements at low velocities. Meanwhile, for higher load velocities, the displacement of poroviscoelastic soils is greater than the viscoelastic [12]. Traffic loads produce a uniform stress distribution (normal and shear) at the tire-pavement interface [13].

The core component of this research is the load cell, which is generally used to calculate the mass of an object and is composed of several conductors, strain gauges, and Wheatstone bridges [14]. Numerous experiments have been conducted on the use and application of load cells. These include making digital scales for Arduino-based rice [15], design and construction of 20kN capacity load cells for Pull and Press workloads on aircraft [16], automatic fruit sorter [17], and the design of an Arduino-based weight and height measurement tool [14]. The vertical displacement and stress in a homogeneous, linearly elastic, isotropic, and infinite soil due to the uniform load on the surface can be determined using the Boussinesq equation [18].

However, in this experiment, the load cell and National Instrument LabVIEW are used to measure the lateral pressure to detect soil movement and shifts caused by vehicles passing through the road on slopes or hills. National Instruments LabVIEW is a graphical programming application specially

created to provide an intuitive programming environment for scientists and engineers [19], [20]. It is similar to a process flow with an interface used to display and retrieve future analysis needs from the system processor.

The vehicle path to be used was determined by conducting sample testing at a certain distance. The height of observation was selected at 3 depth points, namely 0.5 m, 1.0 m, and 1.5 m. The vehicle traversed a straight line at a certain distance from the tool. This study was then aimed to observe the effect of lateral pressure on the sample vehicle to obtain a practical constant in accordance with the observations.

II. THEORY (SOIL MECHANIC)

The basic equation for calculating the pressure is expressed in (1).

$$p = \frac{F}{A} \quad (1)$$

where p = pressure, F = force (kg), and A = cross-sectional area (cm²). The volumetric strain in an elastic material is expressed by (2) [21].

$$\frac{\Delta V}{V} = \frac{1-2\mu}{E} (\sigma_x + \sigma_y + \sigma_z) \quad (2)$$

where, ΔV = volume change, V = initial volume, μ = Poisson ratio, E = elastic modulus, σ_x , σ_y , σ_z = stresses in the x , y , and z directions

In (2), $\Delta V/V$ equals 0 with a Poisson ratio μ of 0.5, supposing the loading that causes a decrease occurs in undrained conditions and at a constant volume. However, $\Delta V/V > 0$, then $\mu < 0.5$ assuming the loading causes a change in volume (such as a decrease due to the consolidation process).

Boussinesq's (1885) theory is used to analyze the stress in the soil mass due to the influence of point loads on the surface [21]. The assumptions used in this theory are as follows:

1. Soil is an elastic, homogeneous, isotropic, and semi-infinite material.
2. It has no weight.
3. The stress-strain relationship is in accordance with Hooke's law.
4. The stress distribution due to the working load does not depend on the type of soil.
5. The stress distribution is symmetric on the vertical (z) axis.
6. Changes in soil volume are negligible.
7. Soil is not under stress before the load Q is applied.

Boussinesq's (1885) theory of additional vertical stress due to point loads is analyzed by considering the stress system in cylindrical coordinates, as shown in Fig. 1. In this theory, the additional vertical stress ($\Delta\sigma_z$) at points A and Q in the soil with a distance (r) and on the surface is expressed by (3) [21].

$$\Delta\sigma_z = -\frac{3Q}{2\pi z^2} \left(\frac{z}{1+(r/z)^2} \right)^{5/2} \quad (3)$$

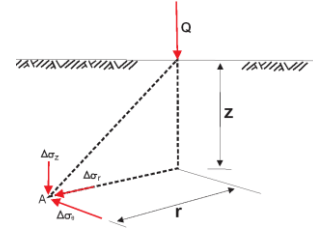


Fig. 1. Additional stress due to point load [21]

Additional horizontal stress in the radial direction ($\Delta\sigma_r$) based on equation (3) can be calculated using (4) [21].

$$\Delta\sigma_r = \frac{Q}{2\pi} \left(\frac{3r^2 z}{(r^2 + z^2)^{5/2}} - \frac{1-2\mu}{r^2 + z^2 + z(r^2 + z^2)^{1/2}} \right) \quad (4)$$

Additional horizontal stress ($\Delta\sigma_\theta$) in the tangential direction is then determined using (3) and (4) obtained the formula [21] expressed as (5).

$$\Delta\sigma_\theta = -\frac{Q}{2\pi} (1-2\mu) \left(\frac{z}{(r^2+z^2)^{3/2}} - \frac{1}{r^2+z^2+z(r^2+z^2)^{1/2}} \right) \quad (5)$$

Meanwhile, shear stress (τ_{rz}) is evaluated based on equations (3), (4) and (5) obtained expression in (6) [21].

$$\tau_{rz} = \frac{3Q}{2\pi} \left(\frac{rz}{(r^2+z^2)^{5/2}} \right) \quad (6)$$

III. METHODOLOGY

The method used to collect pressure data due to lateral ground displacement due to the passage of vehicles at a certain speed is in the form of tool design, measurement methods, flowcharts, and illustrations. for the system flowchart as in Fig. 2.

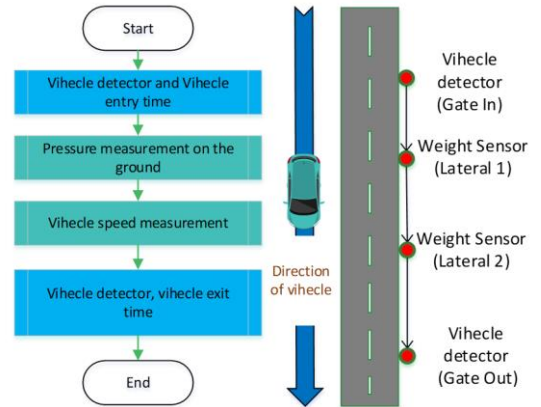


Fig. 2. Flowcharts and experimental illustrations

The tool system starts recording after the vehicle passes the loop detector (Gate In) sensor. Furthermore, the first and second sensors are used to record the results of the soil movement or shift in the form of pressure (Kg/cm²) generated from vehicles passing through the lateral sensors installed beside the track. However, the system stops recording immediately the vehicle passes the loop detector (Gate Out) sensor.

A. Tool Design

The lateral sensors consist of load cells mounted on 2 lateral poles with 3 load cell sensors in 1 lateral pole, as shown in Fig. 3. The measurement results read by the load cell are in the form of weight (Kg), where the results are converted into pressure units.

The lateral sensors are arranged vertically below the soil at a depth point of 50 cm to determine the effect of pressure, as shown in Fig. 4.

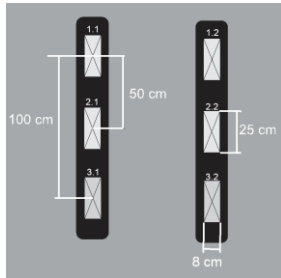


Fig. 3. Lateral Sensor Design

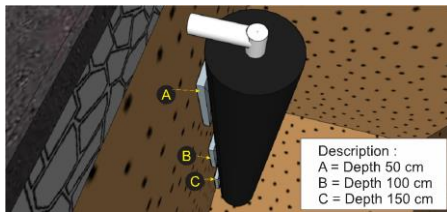


Fig. 4. Placement of the lateral sensor in the soil

B. Measurement Method

1. Pressure measurement

The process of reading the load cell sensor as shown in Fig. 5, produces an analog signal of 0 to 10 volts for a maximum scale, with a capacity of 500 kg. The 0 to 10-volt signal is transmitted to the NI and then processed into a digital signal in the form of a 12-bit ADC (analog-digital converter) value, at a range of 0 – 4096 and 4096 to 500 kg.

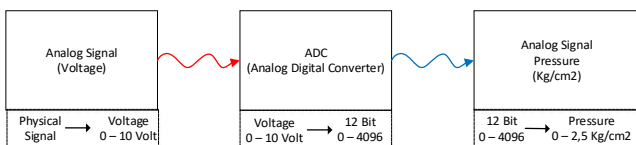


Fig. 5. Process Read Analog Pressure Sensor

The result of the conversion of the analog voltage signal into the ADC value in the NI USB 6008 Then it is converted again into pressure as in (1), and the pressure is obtained at 2.5 kg/cm² for the maximum pressure scale, as shown in Fig. 6.

The conversion results of the analog voltage signal in the ADC value in NI USB 6008 are further converted into pressure by dividing the cross-sectional area by 2.5 kg/cm² for the maximum pressure scale, as shown in Fig. 6.

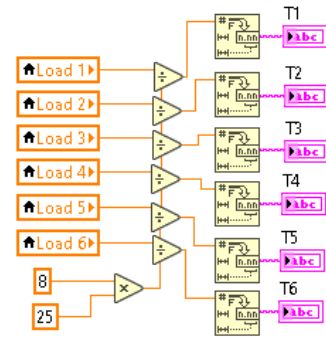


Fig. 6. Labview program converts units of weight to pressure

2. Speed Meter

The vehicle speed is measured using 2 Vehicle Loop Detector sensors installed at the beginning and the end of the circuit, as shown in Fig. 7. This process is used to calculate the time required for the vehicle to travel the test track.

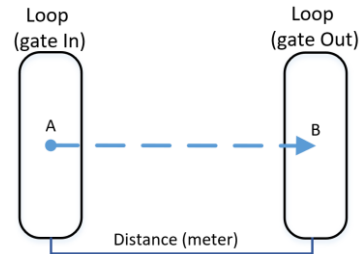


Fig. 7. Vehicle speed measuring method

Fig. 8 is a program snippet from Labview where Sensor Loop (Gate In) turns on the countdown timer, and Sensor Loop (Gate Out) turns off and pauses the timer, therefore the travel time is obtained from Loop (Gate In) to Loop (Gate Out).

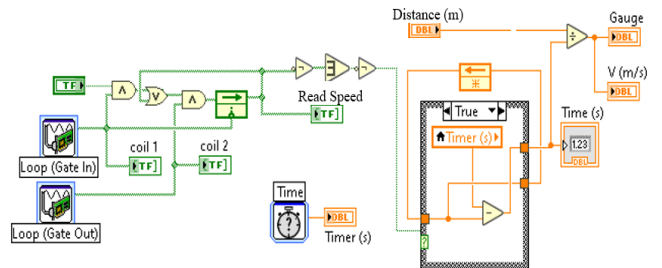


Fig. 8. Vehicle speed meter Labview program

C. Method of data collection

The data collection process is determined from the sampling value of each sensor reading that runs in real-time. Furthermore, the concept of data retrieval and storage is shown in Fig. 9.

Real time analog data that enters the NI USB 6008 is sampled every 10 ms when the sensor is in a state of reading the pressure load and stored in the datalogger in excel format.

Data retrieval on sensor readings is carried out once every 10ms with 100 data collected per second, as shown in Fig. 10. Furthermore, for the data storage process, the reading results are described in Fig. 10 and Fig. 11.

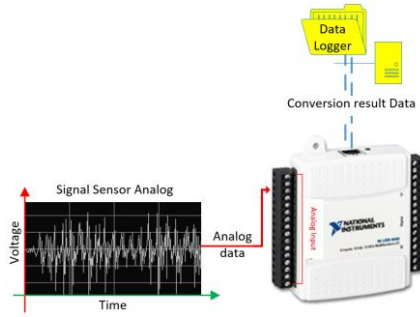


Fig. 9. Experimental data storage method

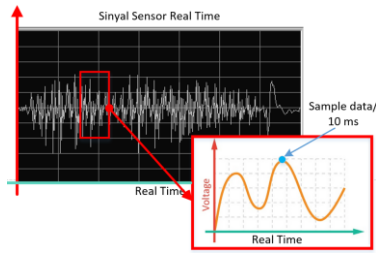


Fig. 10. The sensor data retrieval every 10 ms

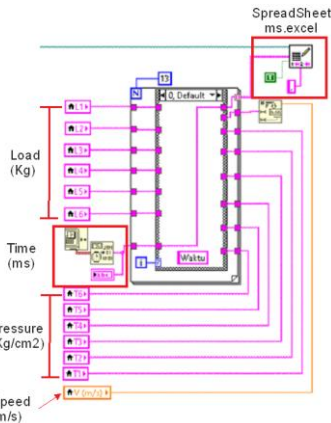


Fig. 11. Labview Program snippet of storing sensor data to datalogger (ms.excel)

D. Testing Method

The test method is carried out by taking some sample parameter data. The first parameter is the distance of the vehicle's wheel trajectory to the sensor device (50 cm, 100 cm and 150 cm distances are used), the second parameter is based on variations in vehicle speed (divided into 3 speed categories; slow, medium and fast), and the third parameter is depth variation (at a depth of 50 cm, 100 cm and 150 cm) Fig. 12. The purpose of this variation is to determine the relationship between the magnitude of the lateral pressure that occurs and its own weight based on the existing theory (Boussinesq).

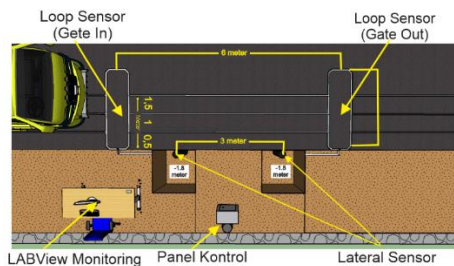


Fig. 12. Testing Method

IV. RESULT AND DISCUSSION

A. Load Cell Sensor calibration results

Before measuring the soil lateral pressure, each sensor is first calibrated by comparing the value read by the load cell sensor with a digital scale, as shown in Fig. 13.

Fig. 13 is a comparison of the measurement results using a load cell sensor and a digital scale. The results showed that the difference read by the load cell is not too far from the digital scale, as illustrated in Table I.

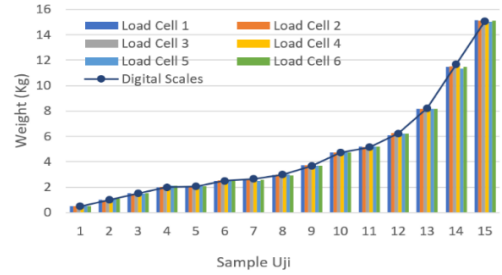


Fig. 13. Comparison graph of load cell measurement results with digital scales

TABLE I. COMPARISON OF LOAD CELL SENSOR READINGS AND DIGITAL SCALES

Sample	Digital Scale (kg)	Sensor Load Cell (Kg)					
		Lateral 1			Lateral 2		
		1	2	3	4	5	6
1	0.50	0.51	0.50	0.52	0.49	0.51	0.51
2	1.00	1.00	0.99	1.03	0.98	1.04	1.09
3	1.50	1.51	1.48	1.53	1.48	1.49	1.50
4	2.00	2.00	2.02	2.10	2.02	2.11	2.10
5	2.07	2.07	2.07	2.07	2.11	2.10	2.09
6	2.50	2.50	2.52	2.48	2.52	2.59	2.51
7	2.66	2.62	2.62	2.59	2.64	2.50	2.59
8	3.00	2.97	2.98	2.92	3.01	2.99	2.90
9	3.66	3.72	3.71	3.72	3.60	3.69	3.70
10	4.73	4.73	4.73	4.71	4.75	4.75	4.75
11	5.16	5.18	5.17	5.19	5.19	5.19	5.19
12	6.23	6.11	6.27	6.21	6.20	6.20	6.21
13	8.23	8.15	8.16	8.21	8.25	8.16	8.16
14	11,66	11.45	11.53	11.61	11.57	11.36	11.45
15	15,07	15.14	15.10	15.11	15.04	15.03	15.11
Avg.	4.66	4.64	4.66	4.67	4.66	4.65	4.66

The comparison of the measurement results through the load cell sensor and digital scales shows that the difference is not too significant. Therefore, the difference in accuracy according to the average results from Table 1 is in the range of ± 0.02 . Fig. 14 shows the real fluctuation of the sample load cell sensor readings.

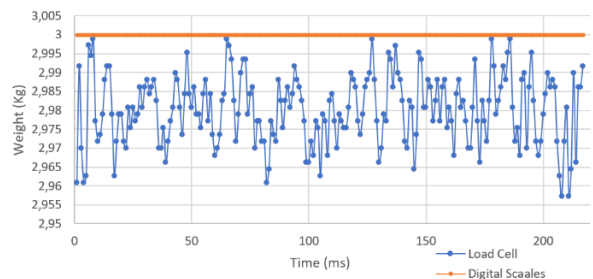


Fig. 14. Real reading of load cell sensor at 3 Kg load

B. Measurement results

The amount of pressure read on the instrument shows the maximum effect according to the theory of static load at the closest distance from the sensor. This is illustrated in Figs. 15 – 17.

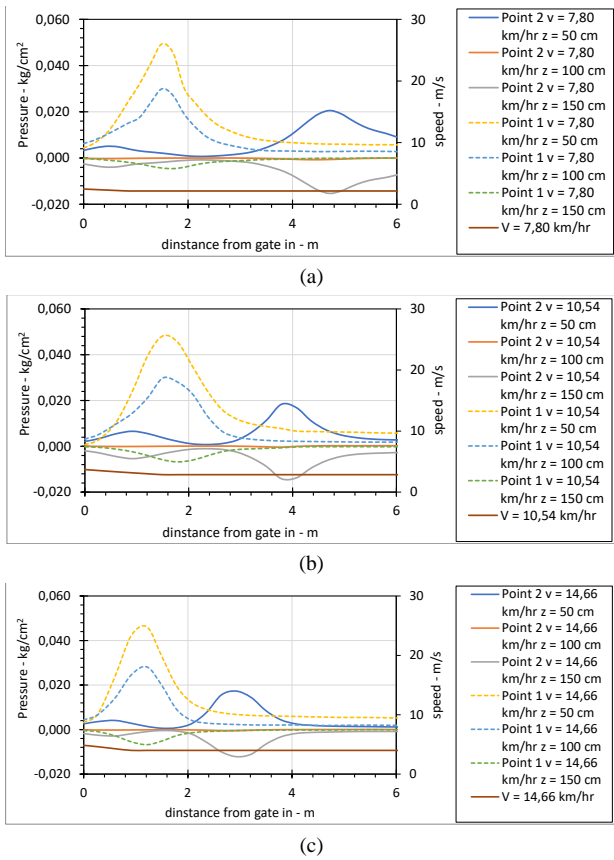


Fig. 15. Lateral pressure at 0.5 m distance from a sensor (location 1), (a) v = 7.8 m/s, (b) v = 10,54 m/s and (c) v = 14,66 m/s

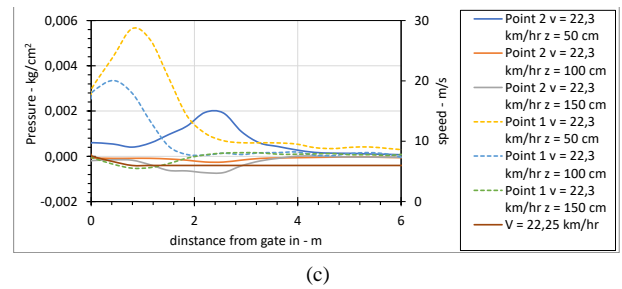
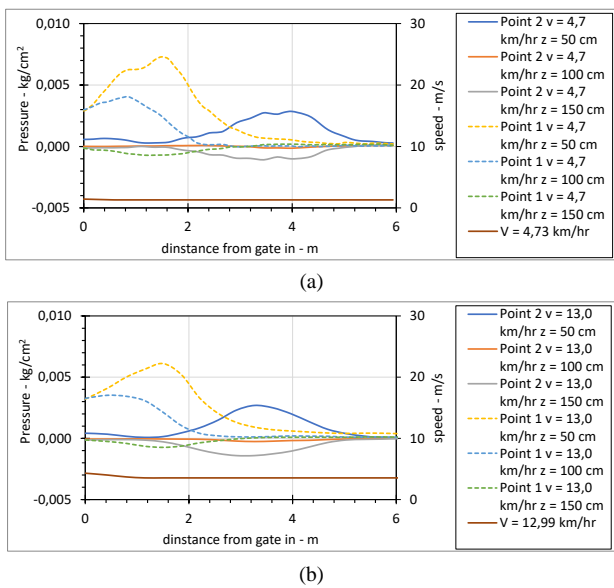


Fig. 16. Lateral pressure at 1.0 m distance from a sensor (location 1), (a) v = 4,73 m/s (b) v = 12,99 m/s and (c) v = 22,25 m/s

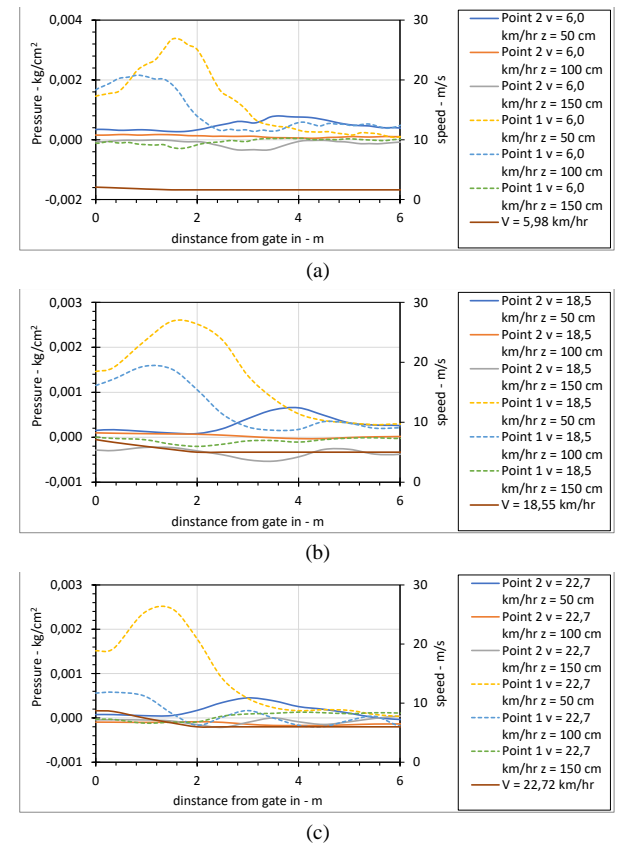
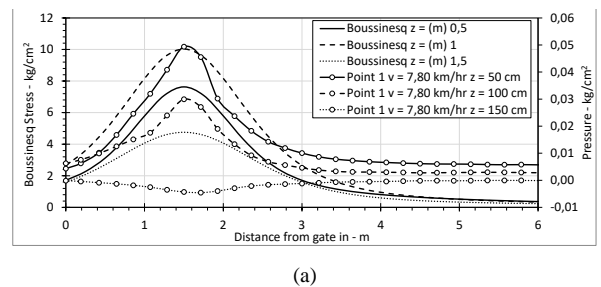


Fig. 17. Lateral pressure at 1.5 m distance from a sensor (location 1), (a) v = 5,98 m/s, (b) v = 18,55 m/s and (c) v = 22,72 m/s

Although the Boussinesq formula is for static loads, the stress distribution that occurs can provide initial information about the stress distribution that occurs in the soil. Fig. 18 shows the comparison between instrumentation data and manual calculations for static loads that have a similar curve pattern.



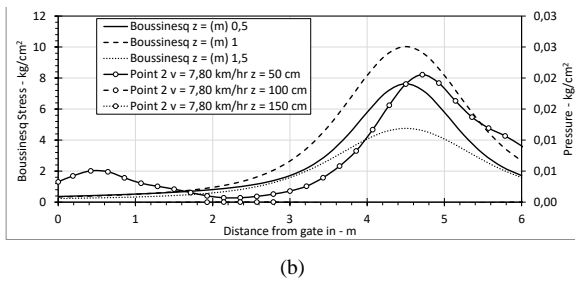


Fig. 18. Comparison of monitoring and Boussinesq calculation results, (a) For left side of lateral sensor (Point 1) and (b) For right side of lateral sensor (Point 2).

The effects of distance based on these data are shown in the curve in Fig. 19 and Fig. 20.

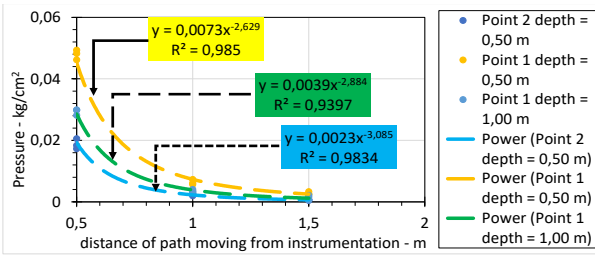


Fig. 19. The influence curve of the load path distance to the instrumentation

As shown in Fig 18, the lateral pressure that occurs is compared with the estimated Boussinesq for a static load at sensor point 1 of about 0.003 times. The influence of vehicle speed on lateral pressure based on the instrumentation results, shown in Fig. 20

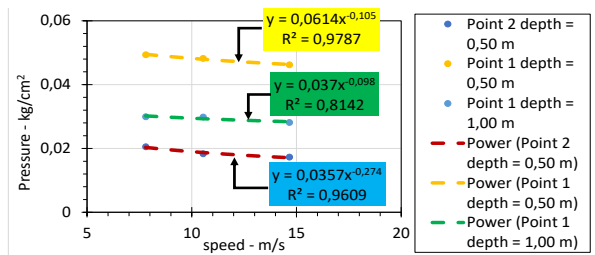


Fig. 20. Relationship between speed and lateral pressure instrumentation results

The curve shows that there is a nonlinear relationship between the distances of the vehicle to the monitoring tool. The further the influence of soil lateral pressure by the running load, the low the pressure. Furthermore, the magnitude of the lateral pressure to the soil also decreases with an increase in vehicle speed.

V. CONCLUSION

The experiment was successful, it can be seen from the curve that has been presented that there is a linear or exponential relationship between the speed and distance of the vehicle to the sensor point. The effect of the load will decrease in proportion to the increase in speed and the increasing distance of the vehicle trajectory from the reference point. It can be seen from the instrumentation results that there is a conformity with the pressure distribution pattern of the Boussinesq formula for stationary loads. Further research needs to be done to obtain an accurate formula for the effect of vehicle speed and distance. For the instrumentation system, it can be improved to avoid the presence of negative pressure

reading at the 1,5 m depth monitoring since it's a non-realistic response in this case.

ACKNOWLEDGMENT

The authors are grateful to the field team for their support and assistance in carrying out this research.

REFERENCES

- [1] M. V. Ivan Vaniček, Daniel Jirásko, *Modern Earth Structures for Transport Engineering_ Engineering and Sustainability Aspects-CRC Press*. Francis: A BALKEMA BOOK, 2020.
- [2] A. K. Agrawal, F. "Frank" Jalinos, N. T. Davis, E. Hoomaan, and M. Sanayei, "Foundation Reuse for Highway Bridges," *DOT Natl. Transp. Integr. Search - ROSA P*, no. November, 2018.
- [3] G. Naresh C. Samtani, "Expanded Database for Service Limit State Calibration of Immediate Settlement of Bridge Foundations on Soil," 2018.
- [4] A. goleman daniel, boyatzis Richard, and Mckee, "Finite element modelling of reinforced road pavements with geogrids J.," *Numer. Methods Geotech. Eng. IX*, vol. 2, pp. 1371–1376, 2018.
- [5] Schiava R, "Numerical simulation of the behavior of collapsible loess," vol. 1, pp. 53–62, 2018.
- [6] A. J. Pytka, "Dynamics of Wheel-Soil Systems A Soil Stress and Deformation-Based Approach," vol. 1, pp. 121–235, 2013.
- [7] G. V. R. Braja M. Das, *Principles of Soil Dynamics, Second Edition*. 2011.
- [8] Braja M. Das & Nagaratnam Sivakugan, *Principles of Foundation Engineering, 9th Edition*. 2019.
- [9] B. M. Das, *Advanced Soil Mechanics*, 5th ed. CRC Press, 2019.
- [10] Qian, G., Jiangu, Q., Xiaoqiang, G. "Dynamic Stress Response of Rough Pavement Resting on Layered Poroelastic Half-Space under Moving Traffic Load," Elsevier, 2017.
- [11] Ming-fu, F., Hai-yan, J., Nab-qing, "Dynamics Response of Ground Vibration due to a Moving Load by using Cole-Cole Model," *Elsevier*, p. 10, 2012.
- [12] Chahour, K., Lefeuvre-Mesgouez, G., Miesgouez, A., Safi, B., "Dynamics Analysis of Multilayered Poroelastoclastic Ground Under a Moving Harmonic Load," *Congres Francais de Mecanique*, 2017.
- [13] Siddhartha R. V., Yao Jian, Sebaaly P. E., "Pavement Strain from Moving Dynamic 3D Load Distribution," *Journal of Transportation Engineering*, 1988.
- [14] M. Afdali, M. Daud, and R. Putri, "Design of a Digital Measurement Tool for Height and Weight with Sound Output based on Arduino UNO," *ELKOMIKA J. Tek. Energi Elektr. Tek. Telekomun. Tek. Elektron.*, vol. 5, no. 1, p. 106, 2018, doi: 10.26760/elkomika.v5i1.106.
- [15] U. Achlison and B. Suhartono, "Analysis of Load Cell Sensor Results for Weighing Rice, Packages and Fruits based on Arduino," vol. 13, no. 1, pp. 96–101, 2020.
- [16] S. W. Sitorus, A. Sudrajat, and K. R. Lestari, "Design and Construction of 20 kN Capacity Load Cells For Tensile and Compressive Work Loads," *J. Ilm. Giga*, vol. 21, no. 1, p. 15, 2019, doi: 10.47313/jig.v21i1.580.
- [17] W. Wahyudi, A. Rahman, and M. Nawawi, "Comparison of Load Cell Sensor Measurement Values on Automatic Fruit Sorter against Manual Scales," *ELKOMIKA J. Tek. Energi Elektr. Tek. Telekomun. Tek. Elektron.*, vol. 5, no. 2, p. 207, 2018, doi: 10.26760/elkomika.v5i2.207.
- [18] Onah, H.N., Mama, B.O., Nwoji, C.U., Ike, C.C., "Boussinesq Displacement Potential Functions Method for Finding Vertical Stresses and Displacement fields due to Distributed load on Elastic Half-Space," *EJGE Vol 22* 2017.
- [19] N. Djermanova, M. Marinov, B. Ganev, S. Tabakov, and G. Nikolov, "LabVIEW based ECG signal acquisition and analysis," 2016 25th Int. Sci. Conf. Electron. 2016.
- [20] A. Izadian, G. Edelman, and S. Johnson, "Gate driver of DC-DC boost converters using national instruments LabVIEW and NImyDAQ," *IEEE Int. Conf. Electro Inf. Technol.*, pp. 530–532, 2014, doi: 10.1109/EIT.2014.6871819.
- [21] Hardiyatmo, H.C., *Soil Mechanics II*, Gadjah Mada University Press, Yogyakarta, 2003.